

## **General Disclaimer**

### **One or more of the Following Statements may affect this Document**

- This document has been reproduced from the best copy furnished by the organizational source. It is being released in the interest of making available as much information as possible.
- This document may contain data, which exceeds the sheet parameters. It was furnished in this condition by the organizational source and is the best copy available.
- This document may contain tone-on-tone or color graphs, charts and/or pictures, which have been reproduced in black and white.
- This document is paginated as submitted by the original source.
- Portions of this document are not fully legible due to the historical nature of some of the material. However, it is the best reproduction available from the original submission.

**NASA Technical Memorandum 82989**

(NASA-TM-82989) INFRARED EMISSION  
SPECTROPHOTOMETRIC STUDY OF THE CHANGES  
PRODUCED BY TiN COATING OF METAL SURFACES IN  
AN OPERATING EHD CONTACT (NASA) 19 p  
HC A02/MF A01

N83-15466

Unclas

CSC 20K G3/27 02432

# **Infrared Emission Spectrophotometric Study of the Changes Produced by TiN Coating of Metal Surfaces in an Operating EHD Contact**

**Leonhard E. Keller and James L. Lauer**  
*Rensselaer Polytechnic Institute*  
*Troy, New York*

and

**William R. Jones, Jr.**  
*Lewis Research Center*  
*Cleveland, Ohio*



Prepared for the  
Joint Lubrication Conference  
cosponsored by the American Society of Lubrication Engineers and the  
American Society of Mechanical Engineers  
Washington, D.C., October 5-7, 1982

**NASA**

INFRARED EMISSION SPECTROPHOTOMETRIC STUDY OF THE CHANGES PRODUCED BY  
TIN COATING OF METAL SURFACES IN AN OPERATING EHD CONTACT

Leonhard E. Keller and James L. Lauer  
Rensselaer Polytechnic Institute  
Department of Mechanical Engineering,  
Aeronautical Engineering and Mechanics  
Troy, New York 12181

and

William R. Jones, Jr.  
National Aeronautics and Space Administration  
Lewis Research Center  
Cleveland, Ohio 44135

E-1398

ABSTRACT

Infrared emission spectra and related measurements were obtained from an operating ball/plate elastohydrodynamic (EHD) sliding contact under a variety of operating conditions. In order to be able to compare the effect of the ball surface, some of the balls were coated with a thin layer of titanium nitride (TiN) by vapor deposition. Polyphenyl ether (5P4E) was used as lubricant and 1 percent of 1,1,2-trichloroethane (TCE) as a surface-probing additive. TiN is chemically inert and its thermal conductivity is lower than that of steel. Therefore, the overall temperatures with TiN-coated balls were higher. Nevertheless, no scuffing was observed with the coated balls under conditions giving rise to scuffing with the uncoated balls. Traction was lower with the TiN-coated balls and always when TCE was added to the 5P4E. These findings were found to be inversely related to the degree of polarization of the spectral emission bands. The intensity and the dichroism of these bands were related to shear rates and inlet conditions of the EHD contact.

INTRODUCTION

In an earlier paper [1],<sup>1</sup> the alignment of lubricant molecules in an elastohydrodynamic (EHD) contact was reported which was deduced from the polarization of the emitted infrared spectrum. With polyphenyl ether (5P4E) as the lubricant, the spectral data were unequivocal in showing that the degree of molecular alignment increased with increasing shear rate and that the addition of 1 percent of 1,1,2-trichloroethane (TCE) increased the alignment substantially. A few preliminary results with titanium nitride (TiN) coated stainless steel balls were also reported; the coating did not seem to affect the alignment significantly.

---

<sup>1</sup> Numbers in brackets designate references at end of paper.

However, during the past year the unique infrared emission Fourier microspectrophotometer was substantially improved. Both accuracy and precision were improved by a new beamsplitter and by computer software changes. Different spectra can now be plotted on the same graph and scale to make comparisons more accurately. Thus, we now have good evidence that TiN-coated bearing balls perform quite differently from uncoated balls, even though the thinness of the coating does not affect the bulk mechanical properties. These differences can be of great technological importance since TiN-coated balls never scuffed or failed in our EHD test rig under conditions where uncoated balls failed.

The objective of this investigation was, therefore, to determine the effects of (1) TiN coatings and (2) additions of a surface active additive (trichloromethane) on the traction, contact temperatures, lubricant alignment, and scuffing characteristics in a ball on plate elastohydrodynamic simulator. Infrared spectra were obtained with a Fourier microspectrophotometer. Conditions included a polyphenyl ether lubricant (5P-4E), 440C stainless steel bearing balls, sliding speeds of 0.6 and 1.2 m/s, Hertzian pressures of 0.6 and 1.2 GPa; and room temperature.

This work was supported by NASA Grant NSG-3170, AFOSR Grant AFOSR-78-3473, and ARO Grant DAAG-29C-0204.

Drs. Hinterman and Boving of Laboratoire Suisse de Recherches Horlogeres helped us obtain the TiN-coated balls.

## EXPERIMENTAL

### Differential Polarization Infrared Emission Fourier Microspectrophotometer for the Analysis of Radiation From a Sliding EHD Contact

Since the instrumentation is basically the same as that described earlier [1], only the essential features and the new improvements will be described. Figure 1 is a schematic drawing of the apparatus, basically a means for accepting and referencing infrared radiation and for analyzing its spectrum by Michelson interferometry. The heated sample shown at the top is represented by a sliding ball/diamond plate EHD contact. A portion of the heat generated in the EHD film is transmitted through the window as infrared radiation. The ball is rotated by a motor-driven shaft about a horizontal axis, while a horizontal platform supported on the ball by rollers is loaded with dead weights. Much of the radiation is captured by a lens below the window. This lens contains only reflecting elements and is thus free from chromatic aberration. Below the lens the radiation passes through a polarizing disc which is driven by a stepping motor. Black and white sectors are painted on the disc to face a lamp/photocell pickup at a predetermined angular position. Varying this position is equivalent to turning the sample about the optic axis of the lens. The pickup provides the reference to the lock-in amplifier to amplify the difference between detector signals, corresponding to a 90° turn of the polarizer, with respect to the reference position. A second stepping motor is used for the Michelson mirror drive. It provides the triggering signal for the A/D converter to read the Golay

angular position. Varying this position is equivalent to turning the sample about the optic axis of the lens. The pickup provides the reference to the lock-in amplifier to amplify the difference between detector signals, corresponding to a  $90^\circ$  turn of the polarizer, with respect to the reference position. A second stepping motor is used for the Michelson mirror drive. It provides the triggering signal for the A/D converter to read the Golay detector output, whenever the Michelson mirror is displaced by a constant increment (usually  $0.5 \mu\text{m}$ ). After passing through the polarizing disc, the beam of radiation is deflected by a small plane mirror into the horizontal plane of the Michelson interferometer, where it enters via the collimator mirror and leaves at the Golay detector. However, there are two more elements ahead of the collimator: a vibrating, tuning-fork-like chopper, and a blackbody source directed toward the chopper tines when they are closed. These elements are not used when the polarizer is used to reference the lock-in amplifier. When the tines are open, radiation from the EHD contact region is detected and when the tines are closed, blackbody radiation is detected. The amplified signal is always a difference between two signals; when the polarizer is used, it is the difference between signals plane-polarized in mutually perpendicular planes, and when the chopper is used, it is the difference between a source signal and a blackbody signal. The source signal can also be polarized by interposition of the polarizing disc in a known, stationary position.

The amplified detector signal is generally recorded as amplitude against Michelson mirror position. It constitutes the so-called interferogram, which is useful for monitoring the instrumental performance, but is not readily interpretable. To obtain a spectrum (i.e., a plot of amplitude against frequency), it must undergo a Fourier transformation.

There are three standard modes of operation: (1) Mode 1, in which only the chopper and the blackbody are used and the spectrum represents the difference between the source radiation and the blackbody radiation; (2) Mode 2, in which only the rotating polarizer is used and the spectrum represents the difference between radiations plane-polarized in two mutually perpendicular planes; and (3) Mode 3, in which the polarizer is held in a fixed position and both the chopper and the blackbody are used. Here the spectrum represents the difference between polarized source radiation and non-polarized blackbody radiation.

The three modes of operation are summarized in Table I. Mode 1 is clearly the mode by which emission spectra are normally obtained. The blackbody reference is needed to remove most of the background of graybody radiation emanating from the contact region. Without the blackbody reference, which must be at about the same temperature as the EHD source, the discrete spectrum of the lubricant would become mere perturbations on a high background and be lost in noise. Mode 2 operation is the most sensitive method of detection because any background radiation and blackbody radiation is randomly polarized and, therefore, subtracted out when only the difference between signals in two polarization planes is amplified. However, it applies only to polarized emission bands. Furthermore, because Mode 2 spectra are differences between discrete spectra, emission bands may appear as absorption bands and the analysis can be difficult. Because the reference direction is determined by the pickup position on the large toothed wheel and can be set, for example, to coincide with the flow direc-

tion in the contact, Mode 2 spectra can be used to analyze lubricant alignment in the contact region. Mode 3 operation can do the same, but is less sensitive than Mode 2. However, it presents the spectra at different angles of polarization and at higher intensity and can, therefore, be used to define molecular alignment more accurately.

### Other Special Apparatus

Thermocouples. The temperature at the diamond window ( $T_D$ ) in the cup holding the test fluid is monitored by a thermocouple, whose junction is attached to that window and buried in the mounting cement. Another thermocouple has its junction in a stagnant location of the cup to measure the average bulk fluid temperature ( $T_B$ ). Of course, the metal surface and fluid temperatures in the contact region can be deduced from the emission spectrum by appropriate calibration [2]. The diamond temperature ( $T_D$ ) measured with the thermocouple is much lower than the true fluid temperature in the contact since the thermocouple is influenced by the surroundings; nevertheless, it is a useful comparative measure.

Traction Measurements. Another ball/plate sliding EHD contact apparatus similar to the one described for infrared emission spectroscopy but with the window on top of the ball instead of below, was built for both traction and film thickness measurements. This device was discussed in an earlier publication [1]. The same bearing balls used in the infrared emission study were used for the traction measurements.

Optical Profilometer. A phase-locked interference microscope, basically a Twyman-Green interferometer with alternating current electronics, capable of a phase resolution of one two hundredth of the wavelength of the red He/Ne laser line ( $6.328 \times 10^{-7}$  m) (6328 Å), was used to obtain the surface profiles of the solid surfaces to ( $\pm 3 \times 10^{-9}$  m) ( $\pm 30$  Å). Changes in surface topography can be recorded with this instrument. This instrument does not require direct contact with the surface measured and has a much smaller effective probe diameter (the 0.6  $\mu$ m laser wavelength compared to a standard 2.5  $\mu$ m stylus diameter of a contacting profilometer) than commonly used profilometers. This instrument was developed by D.T. Moore, et al. [3] at the University of Rochester. A note on our application of it to the study of scuffed-bearing surfaces was published [4] and a more detailed description and results will appear in a separate paper.

### MATERIALS

The bearing balls were  $5.7 \times 10^{-2}$  m (2.25 in.) in diameter and made of 440 C stainless steel. Some were coated with TiN by chemical vapor deposition (CVD) to a uniform thickness of about 4  $\mu$ m as described by Hinterman and Boving [5]. The initial smoothness of all ball surfaces was about 0.01  $\mu$ m (mean asperity height). Since the lubricant film thickness in the EHD contact, under the heaviest load and at the lowest shear rate, was at least 0.5  $\mu$ m as determined earlier [1], asperity interaction was not anticipated to play a role. Both the polyphenyl ether fluid and the 1,1,2-trichloroethane were the same fluids we referred to earlier [1].

## RESULTS

Temperature Measurements. Table II lists the steady state temperature measurements in the EHD contact under various operating conditions. Two speed and two load conditions are shown for both the coated and uncoated balls and for both neat and dilute (1 percent by volume of 1,1,2-trichloroethane, TCE) polyphenyl ether (5P4E). The following observations should be noted:

For 5P4E without TCE,  $T_D$  is higher for the uncoated ball than for the TiN-coated ball; the opposite is true for 5P4E with TCE.  $T_B$  is always lower for the uncoated ball than for the coated ball.

The temperature relations can be shown better when the increases ( $\Delta T = T_D - T_B$ ) are compared in Table III. All the  $\Delta T$ 's are higher for the uncoated ball than for the coated ball, but the differences made by the coating become smaller in the presence of TCE. With the uncoated ball, the presence of TCE causes a relatively large decrease of  $\Delta T$ ; the corresponding decrease with the coated ball is much smaller.

It should be pointed out that equilibrium temperatures in the reservoir partly reflect the heat conducted away at the boundary surfaces of the EHD contact. The cooling coil around the contact in the cup removed the same amount of heat in every experiment, since water from a large thermostated reservoir was pumped through. The bulk temperature ( $T_B$ ) is especially sensitive to the overall thermal losses in the cup. All the heat generated in the cup is from the lubricant sheared in the contact region and essentially all the heat losses are by conduction at the contact boundaries. This mechanism is now well established. Temperature measurements were simultaneous with and in the same apparatus as the spectroscopic measurements.

Traction Measurements. The traction measurements were performed under the same conditions as the spectroscopic measurements, but in the apparatus built specifically for this purpose. As a result, some differences must be expected for these reasons: (a) Instead of a diamond window constituting the plate of the ball/plate sliding contact, a sapphire window was used, and (b) the ball/plate geometry was inverted, with the ball below the plate in the traction apparatus. The main reason for both of these design differences was the space required for the microscope used in determining the lubricant film thickness optically. A large enough diamond for the optical measurements does not warrant the enormous expense. These differences should be only minor, however. The trends should be the same for the two setups.

If we look at the traction results obtained for an intermediate load (Fig. 2), the most outstanding feature is the high traction - ultimately leading to scuffing failure - for the stainless steel ball without the additive. The additive reduced the traction considerably. Scuffing still occurred, but at lower sliding speed. On the other hand, no scuffing occurred with the TiN-coated balls. Here the influence of the additive was small, somewhat reducing traction at low speed, but increasing it at high speed.

Infrared Spectra. Figure 3 shows a Mode 1 reference spectrum from a layer of stationary polyphenyl ether. The intensities of the emission bands depend on temperature, pressure, and polarization. Therefore, they can be quite different for emission spectra from the operating EHD contact, but the position of the bands should be essentially the same.

Briefly, an infrared emission spectrum of an organic compound is a plot of resonances between random thermal motion (i.e., translational motion of the molecules as a whole, and intramolecular vibratory and rotatory motion). For example, the individual atoms in a molecular structure vibrate with respect to their neighbors and, thereby, periodically vary the bond distances and angles slightly. The dipole moments vary with the fundamental normal modes of vibration and other modes and, as in an antenna, corresponding electromagnetic waves are propagated in directional patterns related to the orientation of the varying dipole moment. In any particular orientation, the polarizer will transmit infrared radiation of intensity corresponding to the dipole moment change, generated by a normal mode of vibration or a harmonic or combination mode. The two main emission bands discussed in this section appear at 1110 and 1180  $\text{cm}^{-1}$ . These bands represent in-plane bending vibrations of the aromatic rings of 5P4E. The corresponding transition moments should, therefore, cause radiation to propagate into the interferometer when the rings are aligned parallel to the diamond window.

A very important factor in infrared emission spectroscopy is the constancy of temperature throughout the sample layer. A temperature gradient through the layer can cause reabsorption by colder sublayers of some of the radiation emitted in warmer sublayers and, thus, cause partial or total inversion of emission bands. In other words, emission bands can appear as absorption bands in an emission spectrum [6].

In Figure 4 unpolarized (Mode 1) spectra obtained under high speed/low load conditions from an EHD contact are shown for the two different ball surfaces for the neat and chlorinated lubricant. The major emission bands at 870, 1110, and 1180  $\text{cm}^{-1}$  stand out generally. The last two bands decrease in intensity in the order steel/5P4E, TiN-coated steel/5P4E + TCE, TiN-coated steel/5P4E, and steel/5P4E + TCE. On the other hand, the 870  $\text{cm}^{-1}$  band yields this order: TiN-coated steel/5P4E + TCE, TiN-coated steel/5P4E, steel/5P4E, and steel/5P4E + TCE. In the last case, the band is fully inverted, indicating reabsorption. Some bands are more temperature-sensitive than others, so that reabsorption of one band does not imply reabsorption of all bands. A polarization related to molecular orientation can also come into play.

Comparison of the results for the 1110 and 1180  $\text{cm}^{-1}$  bands, with the entries in Line 3 of Table II for  $T_D$ , shows excellent correspondence with the 1110 and 1180  $\text{cm}^{-1}$  band intensities; conditions giving rise to the highest and lowest  $T_D$ 's, for example, also account for the highest and lowest band intensities. It should further be noted that these  $T_D$ 's and band intensities refer to the uncoated steel ball and 5P4E with and without TCE. The unpolarized spectra corresponding to the entries of the other lines of Table III show similar correspondences.



Polarized infrared emission spectra (Mode 3) obtained under the same conditions as those of Figure 4 for the TiN-coated ball are plotted in Figure 5. These spectra illustrate that the presence of TCE enhances polarization - intensity sequences are more definite (e.g., for the  $1110\text{ cm}^{-1}$  band), - secondly, the maximum and minimum intensities for most bands (but most clearly for the  $1110\text{ cm}^{-1}$  band) occur at  $0^\circ$  and  $90^\circ$  angles of the polarization plane with respect to the Hertzian conjunction plane. The Hertzian conjunction plane is defined as the plane containing the ball/plate contact line and the center of the bearing ball.

Since it is difficult to compare the spectra directly, the plots of Figure 6 were drawn from the data of Figure 5 for the  $1110\text{ cm}^{-1}$  emission band intensities. Assuming the molecular dipole moment change vector corresponding to this band to be about aligned with the Hertzian conjunction plane, turning the polarization plane, with respect to this plane by an angle  $\phi$ , should change the band intensity proportionally to  $\cos^2 \phi$  with half-period of  $90^\circ$ . Since the alignment was not exact, the symmetry of the curves of Figure 6 is not perfect. The curves do show the increased amplitudes produced by the addition of TCE under all four pressure and speed conditions. Furthermore, to show the increased polarization even clearer, a quantitative measure  $P$  - simply the normalized standard deviation of the values plotted in Figure 6 - is tabulated in Table IV for the  $1110\text{ cm}^{-1}$  band. Note that  $P$  is greatest for the highest load and speed and least for the lowest, and that  $P$  is always greater when TCE is present. The reason for the different order of the intermediate  $P$  values with and without TCE is not clear.

That the curves of Figure 6 do not parallel a  $\cos^2 \phi$  wave can be deduced from the inequality of the intensities for  $\phi = +45^\circ$  and  $-45^\circ$  for each set of data. Interestingly, the  $\phi = +45^\circ$  and  $-45^\circ$  intensities are more closely the same when TCE was absent. Mode 2 spectra automatically yield the difference between band intensities in the polarization plane, whose angles with the reference plane differ by  $90^\circ$ . For example, if a plane at  $45^\circ$  from the Hertzian conjunction plane, (i.e.,  $\phi = 45^\circ$ ) were the reference plane, then Mode 2 spectra would give the differences between the values of the intensities shown for  $+45^\circ$  and  $-45^\circ$  in Figure 6. These differences would not be zero for the case of TCE present, but close to zero for TCE absent. Thus TCE not only increases the degree of polarization,  $P$ , and thus the molecular alignment in the EHD contact, but also the direction of the transition moment corresponding to the  $1110\text{ cm}^{-1}$  band as well. In other words, while the projection of this moment in the plane of the polarizer would seem to be coincident with the Hertzian conjunction plane,  $\phi = 0$ , for the highest speed and load when TCE is absent (for then the relative band intensities at  $\phi = +45^\circ$  and  $\phi = -45^\circ$  are equal), it is inclined to this plane when TCE is present.

To pursue this idea further, the Mode 2 data of Figure 7 were plotted for the  $1180\text{ cm}^{-1}$  band from spectra obtained with a TiN-coated ball under the four operating conditions for 5P4E both with and without TCE. It will be noted that the relative band intensities at  $\Delta\phi = -30^\circ$ , corresponding to  $\phi = -30^\circ$  and  $+60^\circ$  with the conjunction plane are minimal and about equal for all conditions with TCE present. This would mean that the projection of the transition moment vector, giving rise to this infrared band, makes an angle  $\phi = +15^\circ$  with the Hertzian conjunction plane. Clearly, the direction

of the transition moment is different when TCE is absent. The  $1180\text{ cm}^{-1}$  band was used to illustrate the Mode 2 experiments because of its earlier identification; however, results were similar for the  $1110\text{ cm}^{-1}$  band. None of the TCE infrared bands will yield emission spectra of this frequency region.

Contour Measurements and Surface Analyses. Contour measurements were performed with the interference microscope before and after the spectroscopic runs. Wear scars found after many hours of running time were deeper and much steeper without the TiN-coating. Furthermore, the uncoated ball contour changes after exposure to an acid medium were much more rapid in the area within the wear scar than outside.

Chlorine found after TCE runs, by energy dispersive X-ray analysis as part of examination by a scanning electron microscope, was generally, but not always, higher in the wear scars. There seems to be evidence - from the interference microscopy - of compound formation and removal. Thus, chemical attack could be a factor aggravating scuffing, and the chemical inertness of the TiN-coating a factor in reducing it. Yet, as was shown, surface temperatures for the coating could be higher because of its relatively low thermal conductivity.

## DISCUSSION

Our reasons for studying the effect of TCE addition were these: (1) organic chlorides are frequent lubricant contaminants from cleaning operations, and (2) chlorides are highly adsorbed, even chemisorbed, on metal surfaces. Since TiN is non-metallic and very inert, TCE addition looked like a good way to study the effect of surface adsorption.

Let us take another look at Table II. According to Hinterman and Boving [5], the thermal conductivity of TiN at 911 K is  $0.088\text{ W/cm K}$  and at 1368 K it is  $0.183\text{ W/cm K}$ . At both of these temperatures, the value for 440 C stainless steel is expected to be at least two to three times higher, and it is reasonable to assume that a similar ratio would hold at our (much lower) experimental temperatures. This would explain the higher  $T_B$ 's when TCE is present: less heat is conducted away by the ball surface.

Higher  $T_B$ 's would imply effectively lower viscosities, thinner EHD films, higher shear rates, and, therefore, higher temperatures at the diamond window ( $T_D$ ) which, in turn, imply higher tractions than those obtained with uncoated steel balls. Actually however, tractions and diamond window temperatures,  $T_D$  were lower (Table I and Fig. 2) with the TiN-coated balls. Indeed, no scuffing occurred with the TiN-coated balls. Furthermore, as Figure 2 also showed, the effects of TCE on traction were much smaller for the TiN-coated balls than for the steel balls. While TCE always reduced traction with the steel balls, TCE also reduced it slightly at low speed and increased it slightly at high speeds with the TiN-coated balls.

These results would seem to be explained only by both a bulk and surface effect ascribable to TCE. Our earlier paper [1] showed that TCE tends to come out of solution at high pressures, resulting in two-phase flow and, thus, a bulk effect. Our present results, comparing the TiN-coated balls

with the steel balls, show definite evidence of a strong surface effect with the steel balls for 5P4E with and without TCE. Only by assuming the existence of such a layer can we account for the higher temperatures generated (the higher  $\Delta T$ 's of Table III) with the uncoated steel balls than with the coated balls, in spite of the formers' higher thermal conductivity. The effective shear rates are higher since the gap, through which the lubricant is flowing, is reduced by the adsorbed layers. Without TCE, the adsorbed layers are 5P4E; with TCE, some of the adsorbed 5P4E is replaced by TCE. This replacement is expected to produce a thinner boundary layer and, therefore, a thicker film of flowing lubricant and a lower film temperature and traction. The latter effect is shown dramatically in Figure 2 when the speed at which scuffing occurred was reduced by TCE by almost 50 percent. The somewhat higher traction caused by TCE at high speeds for both balls, though mostly for the coated ball, would seem to be primarily a bulk effect.

In our previous work, high traction was associated with high temperature rise in the gap, and a comparison of the data of Table III with those of Figure 2 show that this parallelism is true for the present data as well. Clearly the temperature rise,  $\Delta T$ , must be compared, not the initial temperature  $T_g$ . Molecular alignment, as indicated by the extent of polarization, is inversely related to temperature rise and traction. Thus the alignment is greater when the coated ball is substituted for the uncoated ball and the diluted 5P4E for the undiluted, these changes also decreasing traction.

There seems to be little doubt that the molecular alignment, evidenced by the degree of polarization, is largely caused by the shear rate. Thus we are dealing with flow alignment or streaming dichroism. Table IV shows the relationship clearly and Figures 6 and 7 show it as well. The difference in the sequence of increasing  $P$  with and without TCE, in Table IV, is likely to be a bulk effect or two-phase flow in the presence of TCE. Since TCE comes out of solution at high pressure in the contact inlet, as we showed earlier [1], this decreases inlet viscosity and film thickness, thus causing an effectively higher shear rate. The degree of alignment at  $1.2 \text{ ms}^{-1}$  and  $0.6 \text{ GPa}$  is higher in the presence of TCE than in its absence. The degree of alignment of the 5P4E molecules must be determined at the inlet; the more aligned the molecules at the inlet, the faster the flow through the gap. Therefore, the spectrometer, which looks only at the gap, sees a higher degree of flow alignment with the coated balls where the inlet temperatures are higher and, therefore, the viscosities lower.

## SUMMARY OF RESULTS

The results of this study can be summarized as follows:

1. Titanium nitride (TiN)-coated bearing balls did not fail (scuff) under conditions where uncoated 440 C stainless steel balls did.
2. TiN-coated balls yielded lower traction and lower contact temperatures.
3. Addition of trichloroethane (TCE) to the polyphenyl ether always reduced traction with the steel balls. With the TiN-coated balls, TCE slightly reduced traction at low speed, but slightly increased it at high speed.
4. Molecular alignment, as indicated by polarization of infrared emission bands, was found to be inversely related to temperature rise and traction.

## REFERENCES

1. Lauer, J.L., Keller, L.E., Choi, F.H., and King, V.W., "Alignment of Fluid Molecules in an EHD Contact," ASLE Preprint No. 81-LC-5C-1(1981).
2. Lauer, J.L., "Infrared Emission Spectra from Operating Elastohydrodynamic Sliding Contacts," Sun Oil Co., Marcus Hook, PA., Marc, 1976. (NASA CR-134973).
3. Johnson, G.W., Leiner, D.C., and Moore, D.T., "Phase-Locked Interferometry," Optical Engineering, Vol.18, No. 1, Jan.- Feb. 1979, pp. 46-52.
4. Lauer, J.L., Fung, S., and Moore, D.T., "Pit Growth on Scuffed Bearing Surfaces," Bulletin of the American Physical Society, Vol. 27, No. 3, Mar. 1982, p. 226.
5. Hintermann, H.E., and Boving, H., "Wear-Resistant Thin Layers," Die Technik No. 7, 1978, pp 387-395.

TABLE I. - SUMMARY OF OPERATIONAL MODES

Mode	Chopper	Reference	Direction detection
1	Tuning fork	Blackbody with aperture	-----
2	Turning polarizer	Internal	Phase to reference signal
3	Tuning fork	Blackbody with aperture	Static polarizer

TABLE 11. - EHD CONTACT TEMPERATURES

Speed, ms <sup>-1</sup>	Hertzian pressure, GPa	440 C ball				TiN coated ball			
		No additive,		1 Percent TCE		No additive,		1 Percent TCE	
		Diamond temperature, T <sub>D</sub> , °C	Bulk temperature, T <sub>B</sub> , °C	Diamond temperature, T <sub>D</sub> , °C	Bulk temperature, T <sub>B</sub> , °C	Diamond temperature, T <sub>D</sub> , °C	Bulk temperature, T <sub>B</sub> , °C	Diamond temperature, T <sub>D</sub> , °C	Bulk temperature, T <sub>B</sub> , °C
0.6	0.6	53.1	26.8	45.1	22.0	56.0	28.0	47.5	25.0
.6	1.2	63.4	27.2	54.9	23.5	58.5	29.3	54.9	26.2
1.2	.6	56.1	25.6	51.2	23.8	54.9	29.3	52.4	28.6
1.2	1.2	70.8	28.7	61.6	25.6	65.2	31.1	61.9	28.7

ORIGINAL PAGE 13  
OF POOR QUALITY

TABLE III.- TEMPERATURE INCREASES PRODUCED IN THE SLIDING EHD CONTACT

Speed, $\text{ms}^{-1}$	Hertzian pressure, GPa	440 C ball		TiN coated ball	
		No additive	1 Percent TCE	No additive	1 Percent TCE
		Difference between diamond and bulk temperature, $\Delta T$ , $^{\circ}\text{C}$			
0.6	0.6	26.3	23.1	22.0	22.5
.6	1.2	36.2	31.4	29.2	28.7
1.2	.6	30.5	27.4	25.6	23.8
1.2	1.2	42.1	36.0	34.1	33.2

ORIGINAL PAGE IS  
OF POOR QUALITY

TABLE IV. - RELATIVE SPECTAL POLARIZATION OF THE  $1110\text{ cm}^{-1}$  INFRARED EMISSION BAND \* AT VARIOUS OPERATING CONDITIONS OF THE EHD CONTACT WITH THE TiN COATED BALL

Speed, $\text{ms}^{-1}$	Hertzian pressure, GPa	Polarization, P	
		No additive	1 percent TCE
0.6	0.6	0.48	0.68
.6	1.2	.63	.80
1.2	.6	.41	.84
1.2	1.2	.91	1.00

\* Represents in-plane bending of the aromatic polyphenyl ether.

ORIGINAL PAGE IS  
OF POOR QUALITY

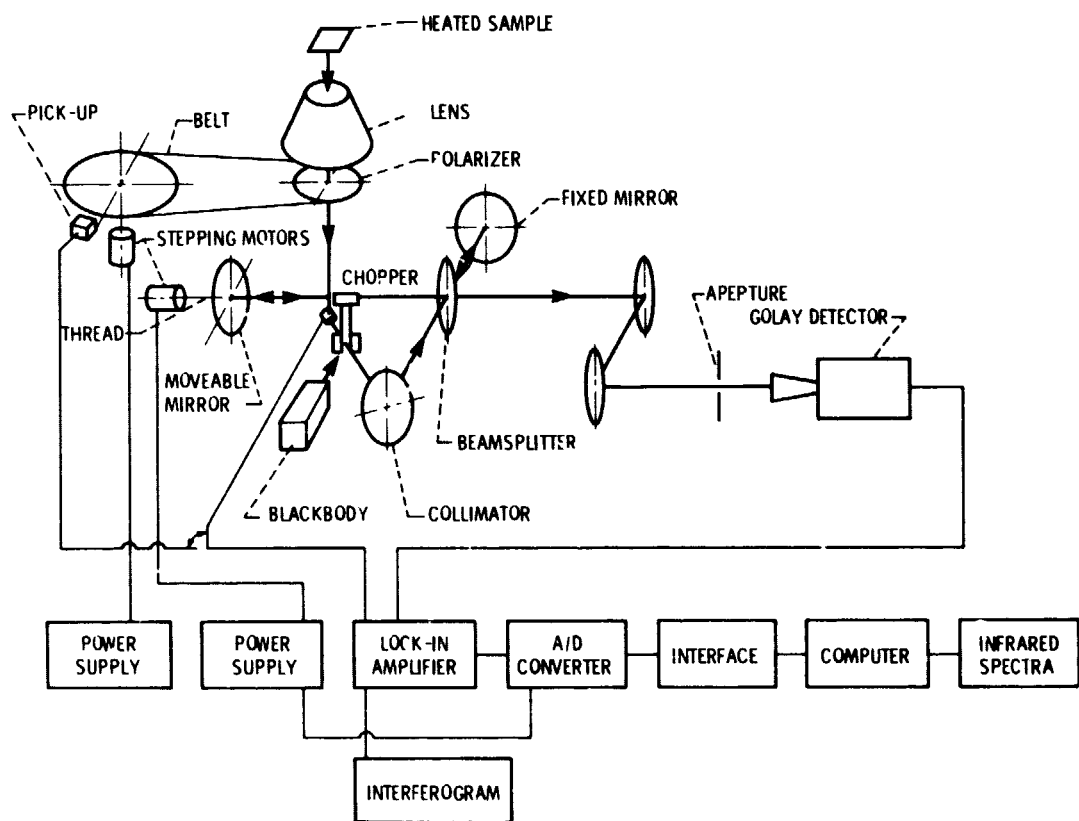


Figure 1. - Schematic drawing of infrared emission fourier microspectrophotometer.



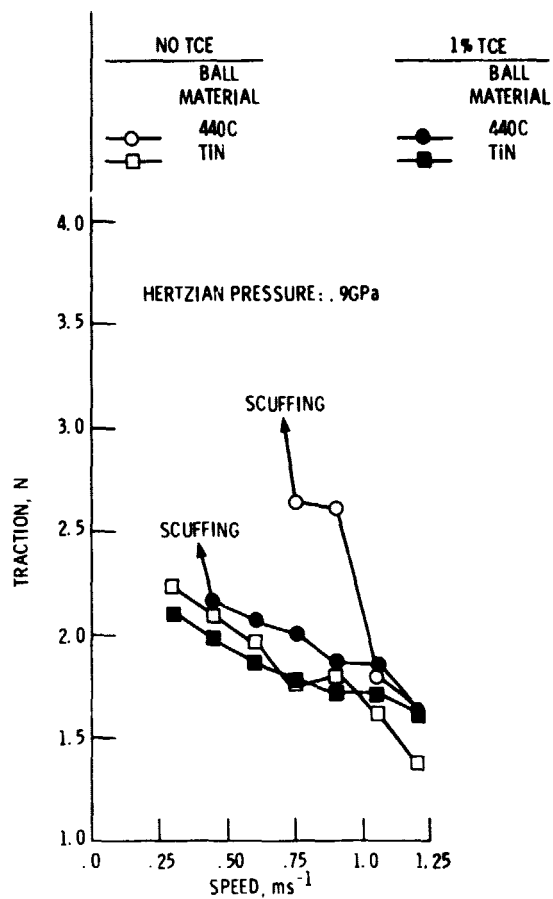


Figure 2. - Relative tractions from an EHD contact with polyphenyl ether (SP4E) with and without 1% 1, 1, 2-trichloroethane by volume.

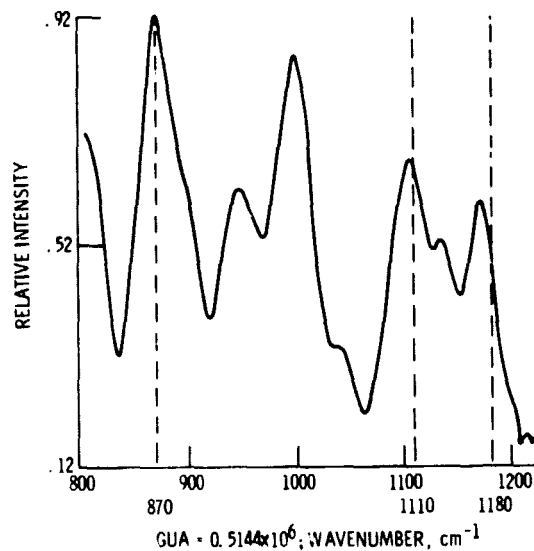


Figure 3. - Infrared emission spectrum of polyphenyl ether (SP4E) under static conditions.

ORIGINAL PAGE IS  
OF POOR QUALITY

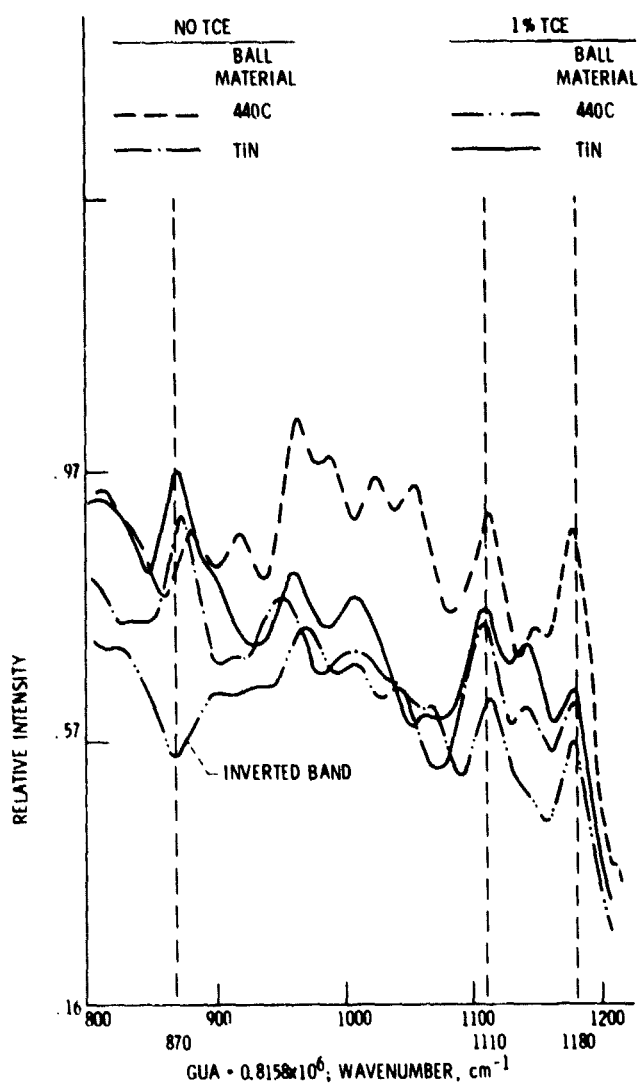


Figure 4 - Comparison of Mode 1, (i.e. unpolarized) emission spectra from a sliding EHD contact (speed:  $1.2 \text{ ms}^{-1}$ ; Hertzian pressure: .6 GPa).